Evasion Strategy of Human Cytomegalovirus to Escape Interferon-β-Induced APOBEC3G Editing Activity

Sara Pautasso,[a] Ganna Galitska,[a] Valentina Dell'Oste,[a] Matteo Biolatti,[a] Rachele Cagliani,[b] Diego Forni,[b] Marco De Andrea, [a,c] Marisa Gariglio,[c] Manuela Sironi,[b] Santo Landolfo,[a#]

[a]Department of Public Health and Pediatric Sciences, University of Turin, Turin, Italy

[b]Scientific Institute IRCCS E. Medea, Bosisio Parini, Italy

[c]Department of Translational Medicine, Novara Medical School, Novara, Italy

Running head: HCMV Escapes APOBEC3G Editing Activity

#Address correspondence to Santo Landolfo, santo.landolfo@unito.it.

Word count abstract: 238

Word count text: 5665

ABSTRACT

The apolipoprotein B editing enzyme catalytic subunit 3 (APOBEC3) is a family of DNA cytosine deaminases that mutate and inactivate viral genomes by single-strand DNA editing, thus providing an innate immune response against a wide range of DNA and RNA viruses. In particular, APOBEC3A (A3A), a member of the APOBEC3 family, is induced by human cytomegalovirus (HCMV) in decidual tissues where it efficiently restricts HCMV replication, thereby acting as an intrinsic innate immune effector at the maternal-fetal interface. However, the widespread incidence of congenital HCMV infection implies that HCMV has evolved to counteract APOBEC3-induced mutagenesis through mechanisms that still remain to be fully established. Here, we have assessed gene expression and deaminase activity of various APOBEC3 gene family members in HCMV-infected primary human foreskin fibroblasts (HFFs). Specifically, we show that APOBEC3G (A3G) and to a lesser degree A3F, but not A3A, gene products are upregulated in HCMV-infected HFFs. We also show that HCMV-mediated induction of A3G expression is mediated by interferon-β (IFN-β), which is produced early during HCMV infection. However, knockout or overexpression of A3G does not affect HCMV replication, indicating that A3G is not a restriction factor for HCMV. Finally, through a bioinformatics approach, we show that HCMV has evolved mutational robustness against IFN-β by limiting the presence of A3G hotspots in essential open reading frames (ORFs) of its genome. Overall, our findings uncover a novel immune evasion strategy by HCMV with profound implications for HCMV infections.

Journal of Virology JVI Journal of Virology

42 **IMPORTANCE**

43 APOBEC3 family of proteins plays a pivotal role in intrinsic immunity defense mechanisms against
44 multiple viral infections, including retroviruses, through the deamination activity. However, the
45 currently available data on APOBEC3 editing mechanisms upon HCMV infection remain unclear.
46 In the present study we show that particularly APOBEC3G (A3G) member of the deaminase family is
47 strongly induced upon infection with HCMV in fibroblasts and its upregulation is mediated by IFN-β.
48 Furthermore, we were able to demonstrate that neither A3G knock out nor its overexpression appear to
49 modulate HCMV replication, indicating that A3G does not inhibit HCMV replication. This may be
50 explained by HCMV escape strategy from A3G activity through depletion of the preferred nucleotide
51 motifs (hotspots) from its genome. The results may shed light on antiviral potential of APOBEC3
52 activity during HCMV infection, as well as the viral counteract mechanisms under A3G-mediated
53 selective pressure.
54

INTRODUCTION

Human cytomegalovirus (HCMV) is a ubiquitous opportunistic β-herpesvirus, which, despite infecting the vast majority of the world's population, can rarely cause symptomatic diseases in healthy, immunocompetent individuals (1). However, reactivation of latent HCMV infection in immunocompromised hosts (e.g. transplant recipients) may result in life-threatening diseases. Likewise, HCMV congenital infection can lead to abortion or dramatic disabilities in the infant including deafness and mental retardation (2). A hallmark of HCMV pathogenesis is its ability to productively replicate in an exceptionally broad range of target cells such as epithelial, smooth muscle and endothelial cells as well as fibroblasts (3, 4).

A central component of innate antiviral immunity against HCMV is the rapid activation of multiple interferon (IFN) signaling pathways that upregulate the expression of a rising number of restriction factors committed to counteract virus replication. Such intrinsic immune mechanisms therefore provide a frontline antiviral defense mediated by constitutively expressed proteins, already present and active before the virus enters a cell (5, 6). These intrinsic immune effectors, which were initially discovered as being active against retroviruses, include the apolipoprotein B editing catalytic subunit-like 3 (APOBEC3) family of cytidine deaminases and tetherin, an IFN-inducible protein whose expression blocks the release of human immunodeficiency virus type 1 (HIV-1) (7). However, it soon became apparent that such effectors were also active against other viruses, such as vesicular stomatitis virus, filoviruses, influenza virus and hepatitis C virus (8). Moreover, other proteins such as PML, hDaxx, Sp100 (9, 10), viperin and IFI16 were subsequently identified as restriction factors mediating the intrinsic immune response against HCMV infection (11, 12).

The seven members of APOBEC3 (A3) family of cytidine deaminases (A, B, C, D, E, F, G and H) (13–16) catalyze the deamination of cytidine nucleotides to uridine nucleotides in single-strand DNA substrates. These enzymes are widely acknowledged as fundamental players in the defense

against various viral infections (14, 15, 17). Since the identification of APOBEC3G (A3G) as a prototype antiretroviral host restriction factor, A3 subsets have been shown to restrict the replication of retroviruses (18), endogenous retroelements (19) and, more recently, DNA viruses such as hepatitis B virus (HBV) (20, 21) and parvoviruses (22, 23). Moreover, different A3 isoforms deaminate human papillomavirus (HPV) genomes (24) as well as BK polyomavirus (BKV) (25). Genomes of some herpesviruses, such as herpes simplex virus-1 (HSV-1) and Epstein-Barr virus (EBV), are edited by APOBEC3 on both strands. Interestingly, the editing is higher on minus strand, possibly due to the fact, that during discontinued replication the lagging strand exposes more viral ssDNA to nuclear APOBEC3s than the leading strand. (14–16, 26). Human APOBEC3 proteins are also able to mutate the genome of the murine Gammaherpesvirus 68 (MHV68) and, therefore, counteract viral replication. In particular, human A3A, A3B and A3C proved their ability to restrict MHV68 replication (27).

With regard to HCMV, Weisblum et al. (28) have recently reported an important role of APOBEC3A (A3A) in mediating innate immunity against congenital HCMV infection. In particular, A3A was strongly upregulated following *ex vivo* HCMV infection of maternal decidua, and overexpression of A3A in epithelial cells hampered HCMV replication by inserting hypermutations into the viral genome through cytidine deamination. A3A induction by HCMV was not observed in HCMV-infected chorionic villi maintained in organ culture, primary human foreskin fibroblasts (HFFs) or epithelial cell cultures, suggesting that HCMV-mediated upregulation of A3A is tissue- and cell-type specific. Intriguingly, IFN-β but not IFN-γ induced A3A expression in uninfected decidual tissues, suggesting its potential regulation as an IFN-stimulated gene during HCMV infection.

However, there still remain a number of issues that need further investigation. For example, in contrast to the aforementioned studies, several reports have demonstrated that members of the A3 family are robustly induced in different cell types *in vitro* and in different tissues *in vivo* either by IFNs or viruses (e.g. HIV and HBV). Thus, the question as to whether HCMV is able to induce other A3

family members besides A3A in different cell types remains open. Another important issue stems from the observation that HCMV triggers IFN production during the early steps of infection, but it is still unclear whether A3 induction is mediated by IFN rather than the virus itself. In this respect, IFN production triggered by HCMV induces expression of IFN-stimulated genes, including the A3 family, which are committed to restrict virus replication as observed in other viral models. Thus, it is conceivable that HCMV has developed strategies to escape from APOBEC3 editing activity. Finally, a major issue concerns APOBEC3 antiviral activity. Although APOBEC3 editing activity has been reported for all the viruses analyzed, it is still a matter of debate whether this is also true for other viruses such as influenza viruses, herpesviruses, papillomaviruses and polyomaviruses. Thus, there is a gap in knowledge concerning the mechanism of HCMV evasion from A3-induced viral genome mutagenesis.

In the present study, we present evidence that: i) A3G and, to a lower extent, A3F gene products are induced in HCMV-infected HFFs; ii) the induction of A3G appears to be mediated by IFN-β as it is drastically decreased upon treatment with anti-IFN type 1 receptor antibodies; iii) neither A3G knock out nor its overexpression appears to modulate HCMV replication, indicating that A3G does not inhibit HCMV replication; and iv) A3G exerted a selective pressure that, during evolution has likely shaped the nucleotide composition of the HCMV genome.

RESULTS

HCMV infection stimulates various APOBEC3 expression patterns in different cell subsets. To assess the role of APOBEC3, we first asked whether HCMV infection could regulate mRNA and protein levels of A3 family members in different cell types. For this purpose, total RNAs from HCMV-infected HFFs, human umbilical vein endothelial cells (HUVECs), macrophages-derived THP-1 or human retinal pigment epithelial (ARPE-19) cells were extracted at 8 and 24 hours post infection (hpi)

and subjected to RT-qPCR analysis. Among all A3 family members analyzed, only A3G and A3F displayed mRNA upregulation in HCMV-infected HFFs compared to mock-infected cells (i.e. ~25 and ~12 fold at 8 hpi; ~10 and ~6 at 24 hpi, respectively) (Fig. 1A). We also observed similar kinetics of mRNA expression for Mx-1, a well-known IFN-inducible gene (Fig. 1A). Human A3F and human A3G share more than 90% promoter sequence similarity and appear to be transcriptionally co-regulated (29, 30). In agreement with these findings, we observed a co-regulated induction of A3G and A3F expression by HCMV. Notably, A3F and A3G were also induced upon HCMV infection in differentiated THP-1, although several other members of APOBEC3 family, namely A3A and A3H, were highly upregulated in this cell line as well. In contrast, mRNA expression levels of all A3 family members including A3G and A3F remained unchanged in HCMV-infected HUVEC and ARPE-19 cells, whereas Mx-1 mRNA was potently induced (Fig. 1B, C), suggesting that induction of A3G and A3F is cell-type specific.

HCMV infection induces A3G in HFFs. Since A3G was the most potently induced A3 family member by HCMV, we decided to focus our attention on this gene in all further analyses. Consistent with the RT-qPCR results (Fig. 1A), A3G protein expression was significantly upregulated in HCMV-infected HFFs (Fig. 2A). Intriguingly, the kinetics of A3G protein induction, which peaked at 72 hpi, were delayed relative to those of A3G mRNA which peaked at 8 hpi (Fig. 1A). At the moment, however, the mechanisms responsible for the delay in protein expression have not been explored. To get further insight into HCMV-induced A3G DNA deaminase activity, we used an *in vitro* fluorescence resonance energy transfer-based oligonucleotide assay (FRET). To this purpose, whole-cell lysates of mock or HCMV-infected HFFs were incubated with a ssDNA oligonucleotide containing a single CCC trinucleotide, which represents the canonical deamination target of A3G, along with uracil-DNA glycosylase (UDG) and RNase A (31). In the presence of A3G cytosine deaminase activity, the formation of a uracil base results in an abasic site following uracil base excision by UDG. Base

hydrolysis of the abasic site then releases an FAM signal from the FRET pair. As expected, protein extracted from HCMV-infected cells displayed deaminase activity consistent with the kinetics of A3G protein induction, reaching a peak at 72 hpi, when the deamination activity was ~5 fold higher than that of mock cells (Fig. 2B). Finally, to verify FRET assay specificity, we included an ssDNA oligonucleotide containing the target motif of A3B (TC) (29) as negative control. As expected, in this case A3G activity was comparable to mock-infected cells, confirming that A3G is selectively activated upon HCMV infection (data not shown).

Collectively, these results show that infection of HFFs with HCMV upregulates A3G DNA deaminase activity in good agreement with the increase of A3G mRNA and protein levels.

Although A3G is typically described as a cytosolic protein (32), several groups have shown that A3G is also present in the nucleus of different cell lines (33–35). To determine whether subcellular A3G localization varies during early and late infection with HCMV, we carried out a detailed kinetic analysis using confocal microscopy at time points ranging from 24 to 72 hpi. HFFs were mock-infected or infected with HCMV at an MOI of 1, and intracellular localization of A3G was assessed by confocal microscopy. Consistent with the Western blot results, a substantial accumulation of A3G in the nucleus of HCMV infected cells was observed at 72 hpi, comparing to the mock-infected cells, where localization of detected A3G seemed evenly distributed among the cytoplasm and nucleus (Fig. 2C). Altogether, these results demonstrate that A3G intranuclear localization is enhanced in HCMV-infected HFFs.

A3G upregulation is IFN-β dependent. The innate immune response against incoming pathogens plays a key role during primary infection, especially in patients with defects in adaptive immunity. Early during infection, HCMV triggers type I IFN production, leading to the induction of a number of IFN-stimulated genes (ISGs), a process that promotes an antiviral state in infected and neighboring cells (36–39). Stimulation of A3 upon IFN production has been observed in different viral models and

cell types (40–44). In particular, A3G is strongly induced by IFN-β in response to influenza A virus infection (43). To assess whether HCMV induces A3G expression through IFN-β induction also in our model, HFFs were incubated for 24 h in the presence of serial dilutions of IFN-β (50-500 U/ml), and the mRNA levels of A3G were determined by RT-qPCR (Fig. 3A). As shown in Fig. 3A, IFN-β stimulation led to over 30-fold induction of A3G mRNA. Likewise, IFN-β treatment of HFFs led to an increase in A3G protein expression over time, which peaked at the 24 h time point (Fig. 3B).

To definitively prove a causative link between IFN-β production and A3G upregulation, HFFs, pre-treated for 18 h with anti-IFNAR antibody (Ab) or an isotype control Ab, were infected with HCMV for 8 h and analyzed by RT-qPCR (Fig. 3C). As expected, suppression of IFN-β production by anti-IFNAR Ab strongly impaired A3G mRNA induction compared to untreated or isotype control Ab-treated HFFs. Altogether, these results indicate that IFN-β released early during HCMV infection triggers A3G expression similarly to what reported for other viruses such as orthomyxoviruses and HPV (43, 44).

HCMV replication is not affected by A3G activity. Several reports have shown that A3G is able to counteract the replication of HIV-1 (45–51), human T-cell lymphotropic virus type 1 (HTLV-1) (52–56) and HBV (20, 21, 57, 58). In contrast, A3 deaminases do not appear to affect viral replication or production of infectious viral progeny of two other viruses such as influenza A (43) virus or polyomavirus (59). Thus, we sought to determine whether A3G acted as a restriction factor for HCMV replication. For this purpose, CRISPR/Cas9 systems were used to knockout A3G gene in HFFs (A3G KO) or scrambled control (Scramble CTRL). Western blot analysis confirmed that the majority of cells were knocked out for A3G. HFFs depleted of A3G were then infected with HCMV at an MOI of 0.1 for 24 h, 72 h, and 144 h, and the viral yield measured by standard plaque assay. As shown in Fig. 4B, the replication of HCMV was not significantly affected following A3G knock out.

198 To further confirm these findings, we transduced HFFs with an adenoviral-derived vector
199 constitutively expressing A3G protein (AdVA3G) or with a control vector (AdVLacZ) at an MOI of
200 30. As shown in Fig. 4C AdVA3G efficiently increased the expression of A3G protein compared to
201 both HCMV or AdVLacZ. After 24 h, cells were infected with HCMV at an MOI of 0.1 for an
202 additional 24 h, 72h, and 144 h and then analyzed by standard plaque assay. The efficiency of A3G
203 mRNA and protein overexpression was monitored by Western blot (Fig 4C). Consistent with the
204 knockout results, A3G overexpression did not exert any antiviral effects on HCMV replication (Fig.
205 4D), indicating either that A3G is not a restriction factor for HCMV replication or, alternatively, that
206 HCMV has evolved to escape A3G restriction activity.
207 **A3G-mediated selective pressure shaped the composition of HCMV genome**. Because HCMV
208 infection upregulates A3G expression with no evidence of virus replication restriction, we sought to
209 determine whether, during evolution, A3G-mediated selective pressure might have played a role in
210 shaping the composition of HCMV genomes.
211 A3G preferentially deaminates the 3' cytosine within CCC hotspots in single-stranded DNA
212 (60, 61), whereas other members of the A3 family have distinct preferences (TTC for A3F and A3C;
213 TC for A3B and A3H; TCG for A3A) (29, 62–67). We thus assessed the representation of these hotspot
214 motifs in the HCMV genome using the HCMV Towne sequence, as a detailed functional map of this
215 strain was constructed by systematic deletion of single open reading frames (ORFs) (68). The
216 representation of CCC:GGG, TTC:GAA, TCG:CGA and TC:GA motifs was calculated in sliding
217 windows and compared to the expected counts obtained by randomly shuffling the HCMV genome
218 sequence (see Methods). Results indicated that the CCC:GGG hotspot is strongly under-represented in
219 several large genomic regions, whereas no such pattern is observed for the other motifs (Fig. 5). In
220 particular, the regions where A3G hotspots are under-represented broadly correspond to the genomic

positions where essential ORFs (i.e. ORFs that impair or strongly reduce HCMV growth *in vitro* when deleted) cluster (68).

To date, only one origin of replication (oriLyt) has been described for HCMV (69). By contrast, the mechanisms of DNA replication remain largely unknown, although a rolling circle phase is likely to occur (70). When we analyzed the frequency of CCC motifs in the two strands of the viral genomes, we detected no substantial difference (Fig. 6A), suggesting that the A3G hotspot under-representation is not mainly determined by preferential deamination of the lagging-strand template (71–74).

Altogether, these observations were consistent with the possibility that HCMV has evolved to limit CCC:GGG motifs in its genome, especially in essential ORFs. To further address this possibility, we used an approach that accounts for the coding capacity of the HCMV genome, as well as for the amino acid composition of single ORFs. In fact, CCC is a codon for proline, and the representation of this hotspot motif in coding genes also depends on the proline content of the encoded proteins. Thus, we counted the frequency of the trinucleotide motifs for A3G, A3A, and A3F/A3C in all HCMV ORFs and obtained expected values by reshuffling codons in each ORF. For each motif in each ORF, we computed a preference index that varies between -1 (under-representation) and +1 (over-representation), with values close to 0 indicating that the representation of motifs is similar to the expected one (see Methods). Analysis of preference indexes indicated that CCC:GGG motifs are under-represented in HCMV ORFs and that the median preference index is well below 0. No such pattern was evident for motifs targeted by other APOBEC3 enzymes, which showed preference indexes close to 0 (Fig. 7A). Also, CCT:AGG motifs, which represent the products of A3G deamination without repair, were not over-represented in HCMV ORFs, and no negative correlation was observed between the preference indexes for CCC:GGG and those for CCT:AGG motifs (Fig. 6B). Thus, the under-representation of A3G motifs is not the result of active A3G-mediated deamination and mutation.

We next sought to determine whether essential and non-essential ORFs displayed a different representation of APOBEC3G motifs. ORFs were categorized based on the mutant growth classification proposed by Dunn and co-workers (68) and preference indexes were compared (see Methods). We found that CCC:GGG motifs are significantly less likely to occur in essential ORFs compared to non-essential ones (Wilcoxon Rank Sum test, p= 0.014) (Fig. 7B). As selective pressure is expected to be stronger at essential ORFs, these latter are the most depleted of A3G motifs.

Finally, we verified that the under-representation of CCC:GGG motifs is a general feature of HCMV genomes and is not limited to the Towne strain. Thus, the preference index for CCC:GGG motifs was calculated for all ORFs of other HCMV strains (including Merlin) and clinical isolates deriving from different sources. No substantial differences were observed between the Towne sequence and any of these strains or isolates (Fig. 7C). Overall, these results suggest that A3G exerted a selective pressure on HCMV and that the virus evolved to limit A3G hotspots in its genome.

DISCUSSION

In summary, we report that HCMV infection specifically upregulates A3G and, to a lesser extent, A3F expression in primary human fibroblasts (HFFs), and that the virus has evolved an escape strategy to avoid editing activity. Our findings indicate that human A3G is induced upon viral infection as a part of the antiviral response mediated by IFN-β. In this regard, addition of anti-IFN receptor Abs during HCMV infection ablates A3G gene product induction demonstrating that A3G induction by HCMV is IFN dependent. Moreover, IFN-β treatment of HFFs can upregulate A3G expression within 24 h in absence of HCMV infection, confirming that A3G is a *bona fide* ISG family member. Accordingly, two IFN-sensitive response elements, namely IFN regulatory factor element (IRF-E)/IFN-stimulated response element (ISRE), located upstream the first A3G exon have been identified (42). Recently, Weisblum et al. (28) found that A3A is strongly upregulated following *ex vivo* HCMV

268 infection of human decidual tissues but not upon infection of chorionic villi, primary fibroblasts (MRC-
269 5 and HFF), and epithelial (ARPE-19) cell cultures. In line with our results, IFN-β significantly
270 induced A3A expression in uninfected decidual tissues, suggesting its potential regulation as an ISG
271 early during HCMV infection. Altogether, these findings demonstrate that A3A and A3G are
272 differentially regulated in HCMV-infected cells.

273 In the same study, Weisblum et al. (28) demonstrated that overexpression of A3A severely
274 impaired HCMV replication in epithelial cells through cytidine deamination of the viral genome.
275 Moreover, exogenous A3A expression in ARPE-19 cells downregulated the expression of viral genes,
276 such as immediate early (IE1) and delayed early (UL89) genes, and reduced HCMV DNA
277 accumulation, suggesting that in this cellular system A3A does restrict virus replication. In contrast to
278 these observations, here we show that neither knock out nor overexpression of A3G can modulate
279 HCMV gene expression and its replication, indicating that A3G does not behave as an HCMV
280 restriction factor *in vitro*.

281 Based on this evidence, we hypothesized that during evolution HCMV might have developed
282 strategies to escape A3G editing activity. To test this hypothesis, we assessed whether A3G-mediated
283 selective pressure shaped the composition of HCMV genomes. A3G preferentially deaminates the 3'
284 cytosine within CCC hotspots in single-stranded DNA, whereas other members of the A3 family have
285 distinct preferences. Notably, the CCC:GGG motif, but not other A3 motifs, was found to be
286 significantly under-represented in several genomic regions where essential ORFs are located. The
287 decrease in CCC:GGG motifs was not paralleled by an increase in their deamination products, and the
288 A3G hotspot motifs were similarly under-represented in both genome strands. Thus, these observations
289 suggest that A3G no longer affects the HCMV genome composition because the virus has likely
290 evolved to limit the presence of A3G hotspot motifs especially within essential ORFs. In this respect, it
291 is worth mentioning that, albeit under-represented, some CCC:GGG motifs do occur in HCMV ORFs,

292 including essential ones. Nevertheless, secondary structures and sequence context are also known to
293 modulate A3G preferences (75), suggesting that extant CCC motifs could represent sub-optimal targets.
294 Our findings are in line with previous studies indicating that target motifs for other A3 enzymes
295 are depleted in the genome of α-papillomaviruses, most likely as the result of viral evolution to avoid
296 restriction (76). Likewise, A3B exerted a selective pressure on BKPyV, which shows an under-
297 representation of hotspot motifs for this enzyme (59). Nonetheless, the specific knockdown of A3B had
298 little short-term effect on productive BKPyV infection (59).
299 Recent results have shown that A3A can restrict HCMV replication in human decidual tissues
300 (28). However, we did not find A3A motifs to be under-represented in HCMV genomes. One possible
301 explanation for this finding is that decidual tissues do not represent the primary target site of HCMV
302 infection and vertical transmission, despite being clinically relevant, does not contribute significantly to
303 HCMV spread in human populations. Thus, the selective pressure exerted by A3A on HCMV may be
304 limited. In fact, we did not find this enzyme to be upregulated by viral infection in HFFs and other
305 primary HCMV target cell types.
306 According to these observations, the following scenario could be envisaged. Early during
307 HCMV infection DNA sensors including cGAS and IFI16 prime IFN-β production, which in turn
308 stimulates expression of ISGs including A3G. To prevent DNA editing by A3G from yielding
309 CCC:GGG hypermutations, the virus has evolved to limit the presence of A3G target motifs in genes
310 essential for its replication.
311 Various strategies have been adopted by different viruses to prevent the catastrophic
312 consequences of A3-induced hypermutations. While several DNA viruses have evolved to limit the
313 availability of A3 target sites (59, 76), HIV has adopted a completely different evasion strategy based
314 on the ability of its protein Vif to bind A3G and promote its degradation through the proteasome
315 pathway (77–80).

316 In conclusion, our studies demonstrate for the first time that: i) early during infection, HCMV
317 upregulates A3G in fibroblasts (HFFs) through IFN-β production; ii) A3G does not restrict HCMV
318 replication, and iii) HCMV has evolved mutational robustness against IFN-β by limiting the presence
319 of A3G hotspots in essential ORFs of its genome. Our findings reveal a novel immune evasion strategy
320 by HCMV, which further fuels its fame as "master in immune evasion".
321
322 **MATERIALS AND METHODS**
323 **Cells and viruses.** Primary human foreskin fibroblasts (HFFs, ATCC SCRC-1041™), human retinal
324 pigment epithelial cells (ARPE-19, ATCC CRL-2302™) and human embryo kidney 293 cells (HEK
325 293, Microbix Biosystems Inc.) were cultured in Dulbecco's Modified Eagle's Medium (Sigma-
326 Aldrich) supplemented with 10% FCS (Sigma-Aldrich) as previously described (81). THP1 cells,
327 cultured as non-adherent monocyte like cells were grown in RPMI (Sigma-Aldrich), with 10% FCS,
328 600 μg/ml Glutamine, 200 IU/ml of penicillin and 100μg/ml streptomycin (Gibco). THP1 cells were
329 differentiated into macrophage like cells by addition of 100nM PMA (Sigma-Aldrich). All presented
330 data with THP1 cells were based on PMA-differentiated cells. Human umbilical vein endothelial cells
331 (HUVECs) were isolated from umbilical veins by chymotrypsin treatment and used for experiments at
332 passage 2±7. HUVECs were cultured in endothelial cell basal medium-2 (EBM-2, Lonza), plus
333 endothelial cell-growth medium supplements (EGM-2, Lonza), FCS (2%, Sigma-Aldrich) and
334 penicillin-streptomycin solution (1%, Sigma-Aldrich). HCMV strain Merlin was kindly provided by
335 Gerhard Jahn (University Hospital of Tübingen, Germany), propagated and titrated on HFFs by
336 standard plaque assay (12, 39).
337 **Recombinant adenoviral vectors.** Adenovirus-derived vectors expressing A3G were generated by
338 means of a replacement strategy using recombineering methods (82). Briefly, the A3G gene was
339 amplified using specific set of primers (Forward: 5'-

AACCGTCAGATCGCCTGGAGACGCCATCCACGCTGTTTTGACCTCCATAGAAGACACCGG GACCGATCCAGCCTGGATCCATGAAGCCTCACTTCAGAAA-3'; Reverse: 5'-TATAGAGTATACAATAGTGACGTGGGATCCCTACGTAGAATCAAGACCTAGGAGCGGGTT AGGGATTGGCTTACCAGCGCTGTTTTCCTGATTCTGGAGA-3'). In order to accomplish homologous recombination, approximately 200 ng of DNA was electroporated into SW102 bacteria harboring pAdZ5-CV5 vector. Cells were then plated on minimal medium agar plates containing 5% sucrose and chloramphenicol and incubated at 32°C for 1 day. The colonies that appeared were inoculated into LB Broth containing ampicillin and chloramphenicol and LB Broth containing chloramphenicol only. In the colonies grown in chloramphenicol only, the A3G ORF replaced the ampicilline resistance sequence in multiple cloning sites. Colonies were checked by PCR and sequencing. To obtain the recombinant adenovirus, the AdZ vector was transfected into HEK 293 packaging cells. Transfected cells were maintained in the 5% CO_2 incubator at 37°C until an extensive cytopathic effect was obtained. Viruses were then purified from infected cultures by freeze-thaw-vortex cycles and assessed for A3G expression by Western blot. For cell transduction, HFFs were washed once with PBS and incubated with AdVA3G at an MOI of 30. After 2 h at 37°C, the virus was washed off and fresh medium applied. For all the experiments, a recombinant adenovirus expressing the E. coli β-galactosidase gene (AdVLacZ) was used as a control (12).

RNA isolation and semiquantitative RT-qPCR. Total RNA was extracted using the NucleoSpin RNA kit (Macherey-Nagel) and 1 µg was retrotranscribed using the Revert-Aid H-Minus FirstStrand cDNA Synthesis Kit (Fermentas), according to the manufacturer's protocol. Comparison of mRNA expression between samples (i.e., infected versus untreated) was performed by SYBR green-based RT-qPCR on a Mx3000P apparatus (Stratagene), using the following primers: A3A Fw: GTCTTATGCCTTCCAATGCC, Rw: GAGAAGGGACAAGCACATGG; A3B Fw: AATGTGTCTGGATCCATCAGG, Rw: TGAAGGTCAGCAATTCATGC; A3C Fw:

364 TCTGCATGACAATGGGTCTC, Rw: AAACTTGGCTGTGCTTCACC; A3D Fw:
365 GATCTGGAAGCGCCTGTTAG, Rw: AGTCGAATCACAGGCAGGAG; A3F Fw:
366 CCATAGGCTTTGCGTAGGTT, Rw: AATTATGCATTCCTGCACCG; A3G Fw:
367 TTCCAAAAGGGAATCACGTC, Rw: AGGGGCTTTCTATGCAACC; A3H Fw:
368 AGCTGTGGCCAGAAGCAC, Rw: CGGAATGTTTCGGCTGTT; GAPDH Fw
369 AGTGGGTGTCGCTGTTGAAGT, Rw AACGTGTCAGTGGTGGACCTG; Mx1 Fw:
370 CCAGCTGCTGCATCCCACCC, Rw AGGGGCGCACCTTCTCCTCA.

371 **Neutralization of type I IFNs.** To neutralize the activity of type I IFNs, specific blocking antibodies
372 against interferon receptor (clone MMHAR-2; Millipore; diluted 1:100) were added to culture media at
373 a concentration of 5 μg/ml for 18 h prior to infection with HCMV Merlin strain, at an MOI of 1, and
374 then left in the supernatant until the end of the respective experiment. Mouse IgG2a (clone MOPC-173;
375 BD Biosciences Europe; diluted 1:100) was used as an isotype control. Human recombinant IFN-β was
376 obtained from PBL (catalog #11415-1).

377 **Transduction of HFFs with lentiviral CRISPR/Cas9.** The CRISPR/Cas9 system was employed to
378 generate specific gene knockouts in primary human fibroblasts. Recombinant lentiviruses were
379 packaged in HEK 293T cells by cotransfection of APOBEC3G sgRNA CRISPR/Cas9 All-in-One
380 Lentivector set (Human) (Applied Biological Materials Inc.) and 2nd Generation Packaging System
381 Mix (Applied Biological Materials Inc.) for producing viral particles using Lipofectamine 2000
382 (Invitrogen). Viral supernatants were harvested after 48 h and used to transduce fibroblasts by infection
383 in the presence of 8 mg/ml Polybrene. Transduced cells were selected with puromycin (1 μg/ml,) over
384 the course of 14 days postransduction. After selection, successful knockout was confirmed using
385 immunoblotting. CRISPR negative control lentivirus were produced with Scrambled sgRNA
386 CRISPR/Cas9 All-in-One Lentivector (Applied Biological Materials Inc.) in HEK293T as described
387 above.

388 **Western blot analysis.** Whole-cell protein extracts were prepared and subject to Western blot analysis
389 as previously described (83, 84). The following primary mouse monoclonal antibodies were used: anti-
390 A3G (VMA00418; Biorad; diluted 1:1000), CMV IEA (CH160; Vyrusis; diluted 1:1000), and α-
391 Tubulin (39527; Active-Motif; diluted 1:4000). Immunocomplexes were detected using sheep anti-
392 mouse antibodies conjugated to horseradish peroxidase (HRP) (GE Healthcare Europe GmbH) and
393 visualized by enhanced chemiluminescence (Super Signal West Pico; Pierce- Thermo Fischer
394 Scientific).

395 **Immunofluorescence microscopy.** Indirect immunofluorescence analysis was performed as
396 previously described (83, 85), using the appropriate dilution of primary antibodies for 1 h at RT in the
397 presence of 10% HCMV negative human serum followed by 1 h incubation with secondary antibodies
398 in the dark at RT. The following primary antibodies were used: rabbit polyclonal anti-CMV IEA
399 antibody (Santo Landolfo, University of Turin; diluted 1:500) or mouse monoclonal antibodies anti-
400 A3G (VMA00418; Biorad; diluted 1:200). Conjugated secondary antibodies included: goat anti-rabbit
401 antibodies Alexa Fluor 568 (A-11011; Life Technologies; diluted 1:200) or goat anti-mouse antibodies
402 Alexa Fluor 488 (R37120; Life Technologies; diluted 1:200). Nuclei were counterstained with 4',6-
403 diamidino-2-phenylindole (DAPI). Finally, coverslips were mounted with Vectashield mounting
404 medium (VECTOR). Samples were observed using a confocal microscope (Leica TCS SP2). ImageJ
405 software was used for image processing.

406 **FRET-based *in vitro* A3G deamination assay.** A fluorescence resonance energy transfer (FRET)
407 based assay was used to detect cytosine deaminase activity of A3G (75). Twenty µl of the cell lysates
408 were used *per* assay using 96 assay plates. A separate solution of 20 pmoles of oligonucleotide, 10 µg
409 RNase A and 0.04 U uracil DNA glycosylase (UDG) were mixed together in 50 mM Tris pH 7.4, 10
410 mM EDTA buffer and adjusted to a total volume of 50 µl, and then transferred to the assay well. The
411 assay plate was then incubated at 37°C for 5 h. Next, 30 µl of 2 M Tris-acetate, pH 7.9 was added to

each well, and the plate was incubated at 95°C for 2 min and on ice for 2.5 min. The fluorescence was then measured at room temperature using a VICTOR^3 1420 Multilabel Counter (Perkin–Elmer). Experiments were conducted with three independent replicates.

Statistical analysis. Statistical tests were performed using GraphPad Prism version 5.00 for Windows (GraphPad Software), unless specified differently in the text. The data were presented as means ± standard deviations (SD). Means between two or three groups were compared by using a one-way or two-way analysis of variance with Bonferroni's post-test. Differences were considered statistically significant for *, $P<0.05$; **, $P<0.01$; ***, $P<0.001$.

Analysis of A3 hotspot motif representation. HCMV genome sequences were obtained from the GenBank database. To evaluate the genomic representation of A3 hotspots, we counted the number of each A3 motif in 1000 bp windows along the HCMV Towne genome, using a sliding window approach with a step of 100 bp, on both genome strands. To assess whether this count is an under- or an over-representation of A3 motifs, we generated 1000 shuffled versions of each window and counted the number of each motif within these windows. The number of these occurrences was then used to create distributions of motif counts (in each window), and the percentile rank of the true motif count was calculated. These percentile ranks are plotted in Fig. 5. For instance, a rank of 0 in a window indicates that the real number of motif counts was lower than all those obtained in reshuffled versions of that same window.

To investigate the distribution of A3G motifs in the HCMV genome by also accounting for coding capacity and amino acid composition, we counted the frequency of motifs in each HCMV ORF. We then obtained expected values by reshuffling codons in each ORF; specifically, for each ORF, we generated 1000 codon-shuffled sequences. We next calculated a preference index for A3 motifs, defined as follows: preference index= (motifs observed-motifs expected)/ (motifs observed + motifs expected). In practical terms, the preference index varies between -1 and +1, with values equal to 0

indicating that the representation of motifs is equal to the expected; negative and positive values indicate under- and over-representation, respectively. ORFs were grouped based on the Mutant Growth Classification proposed by Dunn et. al (68): essential ("no growth" and "severely defective") and non-essential ("moderately defective" and "like wild type").

ACKNOWLEDGEMENTS

This study was supported by: the European Commission under the Horizon2020 program (H2020 MSCA-ITN GA 675278 EDGE); Italian Ministry of Education, University and Research - MIUR (PRIN 2015 to MDA, 2015W729WH; PRIN 2015 to VDO, 2015RMNSTA); Research Funding from the University of Turin 2017 to MDA, SL, and VDO; Associazione Italiana per la Ricerca sul Cancro (AIRC) (IG 2016) to MG. The funders had no role in study design, data collection and interpretation, or the decision to submit the work for publication.

REFERENCES

1. Griffiths P, Baraniak I, Reeves M. 2015. The pathogenesis of human cytomegalovirus. J Pathol 235:288–297.

2. Britt WJ. 2017. Congenital HCMV infection and the enigma of maternal immunity. 91 doi: 10.1128/JVI.02392–16.

3. Gerna G, Revello MG, Baldanti F, Percivalle E, Lilleri D. 2017. The pentameric complex of human Cytomegalovirus: cell tropism, virus dissemination, immune response and vaccine development. J Gen Virol 98:2215–2234.

4. Sinzger C, Digel M, Jahn G. 2008. Cytomegalovirus cell tropism. Curr Top Microbiol Immunol 325:63–83.

459 5. Bieniasz PD. 2004. Intrinsic immunity: a front-line defense against viral attack. Nat Immunol
460 5:1109–1115.

461 6. Roy CR, Mocarski ES. 2007. Pathogen subversion of cell-intrinsic innate immunity. Nat Immunol
462 8:1179–1187.

463 7. Chiu Y-L, Greene WC. 2008. The APOBEC3 cytidine deaminases: an innate defensive network
464 opposing exogenous retroviruses and endogenous retroelements. Annu Rev Immunol 26:317–353.

465 8. Yan N, Chen ZJ. 2012. Intrinsic Antiviral Immunity. Nat Immunol 13:214–222.

466 9. Ahn JH, Hayward GS. 2000. Disruption of PML-associated nuclear bodies by IE1 correlates with
467 efficient early stages of viral gene expression and DNA replication in human cytomegalovirus
468 infection. Virology 274:39–55.

469 10. Tavalai N, Stamminger T. 2009. Interplay between Herpesvirus Infection and Host Defense by
470 PML Nuclear Bodies. Viruses 1:1240–1264.

471 11. Hoek KH, Eyre NS, Shue B, Khantisitthiporn O, Glab-Ampi K, Carr JM, Gartner MJ, Jolly LA,
472 Thomas PQ, Adikusuma F, Jankovic-Karasoulos T, Roberts CT, Helbig KJ, Beard MR. 2017.
473 Viperin is an important host restriction factor in control of Zika virus infection. Sci Rep 7:4475
474 doi: 10.1038/s41598-017-04138-1.

475 12. Gariano GR, Dell'Oste V, Bronzini M, Gatti D, Luganini A, De Andrea M, Gribaudo G, Gariglio
476 M, Landolfo S. 2012. The intracellular DNA sensor IFI16 gene acts as restriction factor for
477 human cytomegalovirus replication. PLoS Pathog 8:e1002498.

478 13. Blanco-Melo D, Venkatesh S, Bieniasz PD. 2012. Intrinsic cellular defenses against human
479 immunodeficiency viruses. Immunity 37:399–411.

480 14. Knisbacher BA, Gerber D, Levanon EY. 2016. DNA Editing by APOBECs: A Genomic Preserver
481 and Transformer. Trends Genet TIG 32:16–28.

482 15. Vieira VC, Soares MA. 2013. The Role of Cytidine Deaminases on Innate Immune Responses
483 against Human Viral Infections. BioMed Res Int 2013:683095 doi: 10.1155/2013/683095.

484 16. Harris RS, Dudley JP. 2015. APOBECs and virus restriction. Virology 479–480:131–145.

485 17. Siriwardena SU, Chen K, Bhagwat AS. 2016. Functions and Malfunctions of Mammalian DNA-
486 Cytosine Deaminases. Chem Rev 116:12688–12710.

487 18. Cullen BR. 2006. Role and mechanism of action of the APOBEC3 family of antiretroviral
488 resistance factors. J Virol 80:1067–1076.

489 19. Refsland EW, Harris RS. 2013. The APOBEC3 family of retroelement restriction factors. Curr
490 Top Microbiol Immunol 371:1–27.

491 20. Turelli P, Mangeat B, Jost S, Vianin S, Trono D. 2004. Inhibition of hepatitis B virus replication
492 by APOBEC3G. Science 303:1829 doi: 10.1126/science.1092066.

493 21. Suspène R, Guétard D, Henry M, Sommer P, Wain-Hobson S, Vartanian J-P. 2005. Extensive
494 editing of both hepatitis B virus DNA strands by APOBEC3 cytidine deaminases in vitro and in
495 vivo. Proc Natl Acad Sci U S A 102:8321–8326.

496 22. Narvaiza I, Linfesty DC, Greener BN, Hakata Y, Pintel DJ, Logue E, Landau NR, Weitzman MD.
497 2009. Deaminase-independent inhibition of parvoviruses by the APOBEC3A cytidine deaminase.
498 PLoS Pathog 5:e1000439.

499 23. Nakaya Y, Stavrou S, Blouch K, Tattersall P, Ross SR. 2016. In Vivo Examination of Mouse
500 APOBEC3- and Human APOBEC3A- and APOBEC3G-Mediated Restriction of Parvovirus and
501 Herpesvirus Infection in Mouse Models. J Virol 90:8005–8012.

502 24. Vartanian J-P, Guétard D, Henry M, Wain-Hobson S. 2008. Evidence for editing of human
503 papillomavirus DNA by APOBEC3 in benign and precancerous lesions. Science 320:230–233.

504 25. Peretti A, Geoghegan EM, Pastrana DV, Smola S, Feld P, Sauter M, Lohse S, Ramesh M, Lim
505 ES, Wang D, Borgogna C, FitzGerald PC, Bliskovsky V, Starrett GJ, Law EK, Harris RS, Killian
506 JK1, Zhu J, Pineda M, Meltzer PS, Boldorini R, Gariglio M, Buck CB. 2018. Characterization of
507 BK Polyomaviruses from Kidney Transplant Recipients Suggests a Role for APOBEC3 in
508 Driving In-Host Virus Evolution. Cell Host Microbe 26: 628-635.

509 26. Suspène R, Aynaud M-M, Koch S, Pasdeloup D, Labetoulle M, Gaertner B, Vartanian J-P,
510 Meyerhans A, Wain-Hobson S. 2011. Genetic Editing of Herpes Simplex Virus 1 and Epstein-
511 Barr Herpesvirus Genomes by Human APOBEC3 Cytidine Deaminases in Culture and In Vivo. J
512 Virol 85:7594–7602.

513 27. Minkah N, Chavez K, Shah P, Maccarthy T, Chen H, Landau N, Krug LT. 2014. Host restriction
514 of murine gammaherpesvirus 68 replication by human APOBEC3 cytidine deaminases but not
515 murine APOBEC3. Virology 454-455:215–226.

516 28. Weisblum Y, Oiknine-Djian E, Zakay-Rones Z, Vorontsov O, Haimov-Kochman R, Nevo Y,
517 Stockheim D, Yagel S, Panet A, Wolf DG. 2017. APOBEC3A is Upregulated by Human
518 Cytomegalovirus in the Maternal-Fetal Interface, Acting as an Innate Anti-HCMV Effector. J
519 Virol 91 doi: 10.1128/JVI.01296–17.

520 29. Bishop KN, Holmes RK, Sheehy AM, Davidson NO, Cho S-J, Malim MH. 2004. Cytidine
521 deamination of retroviral DNA by diverse APOBEC proteins. Curr Biol CB 14:1392–1396.

522 30. Wiegand HL, Doehle BP, Bogerd HP, Cullen BR. 2004. A second human antiretroviral factor,
523 APOBEC3F, is suppressed by the HIV-1 and HIV-2 Vif proteins. EMBO J 23:2451–2458.

524 31. Holtz CM, Sadler HA, Mansky LM. 2013. APOBEC3G cytosine deamination hotspots are
525 defined by both sequence context and single-stranded DNA secondary structure. Nucleic Acids
526 Res 41:6139–6148.

527 32. Stenglein MD, Matsuo H, Harris RS. 2008. Two regions within the amino-terminal half of
528 APOBEC3G cooperate to determine cytoplasmic localization. J Virol 82:9591–9599.

529 33. Lada AG, Waisertreiger IS-R, Grabow CE, Prakash A, Borgstahl GEO, Rogozin IB, Pavlov YI.
530 2011. Replication protein A (RPA) hampers the processive action of APOBEC3G cytosine
531 deaminase on single-stranded DNA. PloS One 6:e24848.

532 34. Nowarski R, Wilner OI, Cheshin O, Shahar OD, Kenig E, Baraz L, Britan-Rosich E, Nagler A,
533 Harris RS, Goldberg M, Willner I, Kotler M. 2012. APOBEC3G enhances lymphoma cell
534 radioresistance by promoting cytidine deaminase-dependent DNA repair. Blood 120:366–375.

535 35. Lackey L, Law EK, Brown WL, Harris RS. 2013. Subcellular localization of the APOBEC3
536 proteins during mitosis and implications for genomic DNA deamination. Cell Cycle Georget Tex
537 12:762–772.

538 36. Abate DA, Watanabe S, Mocarski ES. 2004. Major human cytomegalovirus structural protein
539 pp65 (ppUL83) prevents interferon response factor 3 activation in the interferon response. J Virol
540 78:10995–11006.

541 37. Boehme KW, Singh J, Perry ST, Compton T. 2004. Human cytomegalovirus elicits a coordinated
542 cellular antiviral response via envelope glycoprotein B. J Virol 78:1202–1211.

543 38. Netterwald JR, Jones TR, Britt WJ, Yang S-J, McCrone IP, Zhu H. 2004. Postattachment Events
544 Associated with Viral Entry Are Necessary for Induction of Interferon-Stimulated Genes by
545 Human Cytomegalovirus. J Virol 78:6688–6691.

546 39. Biolatti M, Dell'Oste V, Pautasso S, von Einem J, Marschall M, Plachter B, Gariglio M, De
547 Andrea M, Landolfo S. 2016. Regulatory Interaction between the Cellular Restriction Factor
548 IFI16 and Viral pp65 (pUL83) Modulates Viral Gene Expression and IFI16 Protein Stability. J
549 Virol 90:8238–8250.

550 40. Tanaka Y, Marusawa H, Seno H, Matsumoto Y, Ueda Y, Kodama Y, Endo Y, Yamauchi J,
551 Matsumoto T, Takaori-Kondo A, Ikai I, Chiba T. 2006. Anti-viral protein APOBEC3G is induced
552 by interferon-alpha stimulation in human hepatocytes. Biochem Biophys Res Commun 341:314–
553 319.

554 41. Bonvin M, Achermann F, Greeve I, Stroka D, Keogh A, Inderbitzin D, Candinas D, Sommer P,
555 Wain-Hobson S, Vartanian J-P, Greeve J. 2006. Interferon-inducible expression of APOBEC3

editing enzymes in human hepatocytes and inhibition of hepatitis B virus replication. Hepatol Baltim Md 43:1364–1374.

42. Peng G, Lei KJ, Jin W, Greenwell-Wild T, Wahl SM. 2006. Induction of APOBEC3 family proteins, a defensive maneuver underlying interferon-induced anti–HIV-1 activity. J Exp Med 203:41–46.

43. Pauli E-K, Schmolke M, Hofmann H, Ehrhardt C, Flory E, Münk C, Ludwig S. 2009. High level expression of the anti-retroviral protein APOBEC3G is induced by influenza A virus but does not confer antiviral activity. Retrovirology 6:38 doi: 10.1186/1742-4690-6-38.

44. Wang Z, Wakae K, Kitamura K, Aoyama S, Liu G, Koura M, Monjurul AM, Kukimoto I, Muramatsu M. 2014. APOBEC3 Deaminases Induce Hypermutation in Human Papillomavirus 16 DNA upon Beta Interferon Stimulation. J Virol 88:1308–1317.

45. Apolonia L, Schulz R, Curk T, Rocha P, Swanson CM, Schaller T, Ule J, Malim MH. 2015. Promiscuous RNA binding ensures effective encapsidation of APOBEC3 proteins by HIV-1. PLoS Pathog 11:e1004609.

46. Bogerd HP, Cullen BR. 2008. Single-stranded RNA facilitates nucleocapsid: APOBEC3G complex formation. RNA 14:1228–1236.

47. Strebel K, Khan MA. 2008. APOBEC3G encapsidation into HIV-1 virions: which RNA is it? Retrovirology 5:55 doi: 10.1186/1742-4690-5-55.

48. Tian C, Wang T, Zhang W, Yu X-F. 2007. Virion packaging determinants and reverse transcription of SRP RNA in HIV-1 particles. Nucleic Acids Res 35:7288–7302.

576 49. Wang T, Tian C, Zhang W, Luo K, Sarkis PTN, Yu L, Liu B, Yu Y, Yu X-F. 2007. 7SL RNA
577 mediates virion packaging of the antiviral cytidine deaminase APOBEC3G. J Virol 81:13112–
578 13124.

579 50. Wang T, Zhang W, Tian C, Liu B, Yu Y, Ding L, Spearman P, Yu X-F. 2008. Distinct viral
580 determinants for the packaging of human cytidine deaminases APOBEC3G and APOBEC3C.
581 Virology 377:71–79.

582 51. Zhen A, Du J, Zhou X, Xiong Y, Yu X-F. 2012. Reduced APOBEC3H variant anti-viral activities
583 are associated with altered RNA binding activities. PloS One 7:e38771.

584 52. Derse D, Hill SA, Princler G, Lloyd P, Heidecker G. 2007. Resistance of human T cell leukemia
585 virus type 1 to APOBEC3G restriction is mediated by elements in nucleocapsid. Proc Natl Acad
586 Sci U S A 104:2915–2920.

587 53. Mahieux R, Suspène R, Delebecque F, Henry M, Schwartz O, Wain-Hobson S, Vartanian J-P.
588 2005. Extensive editing of a small fraction of human T-cell leukemia virus type 1 genomes by
589 four APOBEC3 cytidine deaminases. J Gen Virol 86:2489–2494.

590 54. Ooms M, Krikoni A, Kress AK, Simon V, Münk C. 2012. APOBEC3A, APOBEC3B, and
591 APOBEC3H haplotype 2 restrict human T-lymphotropic virus type 1. J Virol 86:6097–6108.

592 55. Sasada A, Takaori-Kondo A, Shirakawa K, Kobayashi M, Abudu A, Hishizawa M, Imada K,
593 Tanaka Y, Uchiyama T. 2005. APOBEC3G targets human T-cell leukemia virus type 1.
594 Retrovirology 2:32 doi. 10.1186/1742-4690-2-32.

595 56. Strebel K. 2005. APOBEC3G & HTLV-1: inhibition without deamination. Retrovirology 2:37
596 doi: 10.1186/1742-4690-2-37.

57. Vartanian J-P, Henry M, Marchio A, Suspène R, Aynaud M-M, Guétard D, Cervantes-Gonzalez M, Battiston C, Mazzaferro V, Pineau P, Dejean A, Wain-Hobson S. 2010. Massive APOBEC3 editing of hepatitis B viral DNA in cirrhosis. PLoS Pathog 6:e1000928.

58. Beggel B, Münk C, Däumer M, Hauck K, Häussinger D, Lengauer T, Erhardt A. 2013. Full genome ultra-deep pyrosequencing associates G-to-A hypermutation of the hepatitis B virus genome with the natural progression of hepatitis B. J Viral Hepat 20:882–889.

59. Verhalen B, Starrett GJ, Harris RS, Jiang M. 2016. Functional Upregulation of the DNA Cytosine Deaminase APOBEC3B by Polyomaviruses. J Virol 90:6379–6386.

60. Yu Q, König R, Pillai S, Chiles K, Kearney M, Palmer S, Richman D, Coffin JM, Landau NR. 2004. Single-strand specificity of APOBEC3G accounts for minus-strand deamination of the HIV genome. Nat Struct Mol Biol 11:435–442.

61. Chelico L, Pham P, Calabrese P, Goodman MF. 2006. APOBEC3G DNA deaminase acts processively 3' --> 5' on single-stranded DNA. Nat Struct Mol Biol 13:392–399.

62. Liddament MT, Brown WL, Schumacher AJ, Harris RS. 2004. APOBEC3F properties and hypermutation preferences indicate activity against HIV-1 in vivo. Curr Biol CB 14:1385–1391.

63. Armitage AE, Deforche K, Welch JJ, Van Laethem K, Camacho R, Rambaut A, Iversen AKN. 2014. Possible footprints of APOBEC3F and/or other APOBEC3 deaminases, but not APOBEC3G, on HIV-1 from patients with acute/early and chronic infections. J Virol 88:12882–12894.

64. Taylor BJ, Nik-Zainal S, Wu YL, Stebbings LA, Raine K, Campbell PJ, Rada C, Stratton MR, Neuberger MS. 2013. DNA deaminases induce break-associated mutation showers with

implication of APOBEC3B and 3A in breast cancer kataegis. eLife 2:e00534 doi:10.7554/eLife.00534.

65. Hultquist JF, Lengyel JA, Refsland EW, LaRue RS, Lackey L, Brown WL, Harris RS. 2011. Human and rhesus APOBEC3D, APOBEC3F, APOBEC3G, and APOBEC3H demonstrate a conserved capacity to restrict Vif-deficient HIV-1. J Virol 85:11220–11234.

66. Yu Q, Chen D, König R, Mariani R, Unutmaz D, Landau NR. 2004. APOBEC3B and APOBEC3C are potent inhibitors of simian immunodeficiency virus replication. J Biol Chem 279:53379–53386.

67. Shi K, Carpenter MA, Banerjee S, Shaban NM, Kurahashi K, Salamango DJ, McCann JL, Starrett GJ, Duffy JV, Demir Ö, Amaro RE, Harki DA, Harris RS, Aihara H. 2017. Structural basis for targeted DNA cytosine deamination and mutagenesis by APOBEC3A and APOBEC3B. Nat Struct Mol Biol 24:131–139.

68. Dunn W, Chou C, Li H, Hai R, Patterson D, Stolc V, Zhu H, Liu F. 2003. Functional profiling of a human cytomegalovirus genome. Proc Natl Acad Sci U S A 100:14223–14228.

69. Zhu Y, Huang L, Anders DG. 1998. Human cytomegalovirus oriLyt sequence requirements. J Virol 72:4989–4996.

70. Boehmer PE, Nimonkar AV. 2003. Herpes virus replication. IUBMB Life 55:13–22 doi: 10.1080/1521654031000070645

71. Seplyarskiy VB, Soldatov RA, Popadin KY, Antonarakis SE, Bazykin GA, Nikolaev SI. 2016. APOBEC-induced mutations in human cancers are strongly enriched on the lagging DNA strand during replication. Genome Res 26:174–182.

639 72. Hoopes JI, Cortez LM, Mertz TM, Malc EP, Mieczkowski PA, Roberts SA. 2016. APOBEC3A
640 and APOBEC3B Preferentially Deaminate the Lagging Strand Template during DNA Replication.
641 Cell Rep 14:1273–1282.

642 73. Haradhvala NJ, Polak P, Stojanov P, Covington KR, Shinbrot E, Hess JM, Rheinbay E, Kim J,
643 Maruvka YE, Braunstein LZ, Kamburov A, Hanawalt PC, Wheeler DA, Koren A, Lawrence MS,
644 Getz G. 2016. Mutational Strand Asymmetries in Cancer Genomes Reveal Mechanisms of DNA
645 Damage and Repair. Cell 164:538–549.

646 74. Seplyarskiy VB, Andrianova MA, Bazykin GA. 2017. APOBEC3A/B-induced mutagenesis is
647 responsible for 20% of heritable mutations in the TpCpW context. Genome Res 27:175–184.

648 75. Holtz CM, Sadler HA, Mansky LM. 2013. APOBEC3G cytosine deamination hotspots are
649 defined by both sequence context and single-stranded DNA secondary structure. Nucleic Acids
650 Res 41:6139–6148.

651 76. Warren CJ, Van Doorslaer K, Pandey A, Espinosa JM, Pyeon D. 2015. Role of the host restriction
652 factor APOBEC3 on papillomavirus evolution. Virus Evol 1 doi: 10.1093/ve/vev015.

653 77. Marin M, Rose KM, Kozak SL, Kabat D. 2003. HIV-1 Vif protein binds the editing enzyme
654 APOBEC3G and induces its degradation. Nat Med 9:1398–1403.

655 78. Sheehy AM, Gaddis NC, Malim MH. 2003. The antiretroviral enzyme APOBEC3G is degraded
656 by the proteasome in response to HIV-1 Vif. Nat Med 9:1404–1407.

657 79. Stopak K, de Noronha C, Yonemoto W, Greene WC. 2003. HIV-1 Vif blocks the antiviral activity
658 of APOBEC3G by impairing both its translation and intracellular stability. Mol Cell 12:591–601.

80. Yu X, Yu Y, Liu B, Luo K, Kong W, Mao P, Yu X-F. 2003. Induction of APOBEC3G ubiquitination and degradation by an HIV-1 Vif-Cul5-SCF complex. Science 302:1056–1060.

81. Baggetta R, De Andrea M, Gariano GR, Mondini M, Rittà M, Caposio P, Cappello P, Giovarelli M, Gariglio M, Landolfo S. 2010. The interferon-inducible gene IFI16 secretome of endothelial cells drives the early steps of the inflammatory response. Eur J Immunol 40:2182–2189.

82. Chartier C, Degryse E, Gantzer M, Dieterle A, Pavirani A, Mehtali M. 1996. Efficient generation of recombinant adenovirus vectors by homologous recombination in Escherichia coli. J Virol 70:4805–4810.

83. Dell'Oste V, Gatti D, Gugliesi F, De Andrea M, Bawadekar M, Lo Cigno I, Biolatti M, Vallino M, Marschall M, Gariglio M, Landolfo S. 2014. Innate Nuclear Sensor IFI16 Translocates into the Cytoplasm during the Early Stage of In Vitro Human Cytomegalovirus Infection and Is Entrapped in the Egressing Virions during the Late Stage. J Virol 88:6970–6982.

84. Gugliesi F, Mondini M, Ravera R, Robotti A, de Andrea M, Gribaudo G, Gariglio M, Landolfo S. 2005. Up-regulation of the interferon-inducible IFI16 gene by oxidative stress triggers p53 transcriptional activity in endothelial cells. J Leukoc Biol 77:820–829.

85. Biolatti M, Dell'Oste V, Pautasso S, Gugliesi F, von Einem J, Krapp C, Jakobsen MR, Borgogna C, Gariglio M, De Andrea M, Landolfo S. 2017. The Human Cytomegalovirus Tegument Protein pp65 (pUL83) Dampens Type I Interferon Production by Inactivating the DNA Sensor cGAS without Affecting STING. J Virol. pii: JVI.01774–17 doi: 10.1128/JVI.01774-17.

FIGURE LEGENDS

680 **FIG 1** Apolipoprotein B editing enzyme catalytic subunit 3 (APOBEC3) gene expression patterns in
681 human cytomegalovirus (HCMV)-infected cells. Primary human foreskin fibroblasts (HFFs) (A),
682 human umbilical vein endothelial cells (HUVECs) (B), differentiated THP1-1 cells (THP-1
683 macrophages) (C) or human retinal pigment epithelial cells (ARPE-19) (D) were infected with HCMV
684 at an MOI of 1 and subject to RT-qPCR to measure mRNA expression of various APOBEC3 family
685 members (i.e. A3A, A3B, A3C, A3DE, A3F, A3G and A3H) and Mx-1. Values were normalized to the
686 housekeeping gene glyceraldehyde-3-phosphate dehydrogenase (GAPDH) mRNA, and plotted as a
687 fold induction relative to mock-infected cells. Data are presented as mean values of biological
688 triplicates. Error bars show standard deviations, (*, P< 0.05; **, P< 0.01; one-way ANOVA followed
689 by Bonferroni's post-tests, for comparison of infected versus mock cells).
690
691 **FIG 2** HCMV infection upregulates A3G in HFFs. (A) Lysates were prepared at the indicated time-
692 points and subject to Western blot analysis for A3G, IEA and α-Tubulin (left panel). A3G protein was
693 subject to densitometry and normalized to α-Tubulin (*, P< 0.05; ***, P< 0.001; one-way ANOVA
694 followed by Bonferroni's post-tests, for comparison of infected versus mock cells) (right panel). (B)
695 FRET assay to measure A3G deaminase activity. The average and standard deviation were calculated
696 from three independent experiments (**, P< 0.01; ***, P< 0.001; one-way ANOVA followed by
697 Bonferroni's post-tests, for comparison of infected versus mock cells). RFU, relative fluorescence
698 units. (C) HFFs were infected with HCMV at an MOI of 1, or left uninfected (mock) and subject to
699 immunofluorescence analysis at the indicated time-points. A3G (green)/IEA (red) were visualized
700 using primary antibodies followed by secondary antibody staining in the presence of 10% HCMV-
701 negative human serum. Nuclei were counterstained with DAPI (blue). Images were acquired at X63
702 magnification, and representative pictures are shown.
703

704 **FIG 3** APOBEC3G upregulation is IFN-β dependent. (A) HFFs were stimulated for 24 h with the
705 indicated doses of IFN-β, and the mRNA levels of A3G were determined by means of RT-qPCR.
706 Values were normalized to GAPDH mRNA and plotted as fold induction relative to untreated HFFs.
707 (B) Western blot analysis to assess APOBEC3G protein levels and α-Tubulin upon IFN-β treatment
708 (1000 U/ml) for the indicated time points (hpt, hours post treatment). One representative experiment of
709 three performed in duplicate is shown. (C) HFFs were mock- and HCMV-infected in the presence of an
710 anti-IFNAR antibody (5 µg/ml) or isotype control. At 8 hpi, cells were processed by RT-qPCR to
711 assess A3G expression. Data presented in (A) and (C) are mean values of biological triplicates. Error
712 bars show standard deviations (*, P< 0.05; **, P< 0.01; one-way ANOVA followed by Bonferroni's
713 post-tests, for comparison of treated versus untreated cells).
714
715 **FIG 4** A3G is not a restriction factor for HCMV replication. (A) Knockout gene variants in HFFs for
716 A3G (A3G KO) and the scramble control, were generated with CRISPR-Cas9 technology. The
717 efficiency of A3G depletion was measured by Western blot analysis for A3G and α-Tubulin. (B) A3G
718 KO HFFs were infected with HCMV at an MOI of 0.1. The extent of virus replication was measured at
719 the indicated times post-infection by titrating the infectivity of supernatants and cell suspension on
720 HFFs by standard plaque assay. Results are expressed as means ± SD. (C) HFFs were transduced with
721 AdVA3G or AdVLacZ at an MOI of 30 PFU/cell. The efficiency of A3G overexpression was measured
722 by Western blot analysis for A3G and α-Tubulin. (D) HFFs were transduced with AdV vectors as
723 described in (C). Subsequently, cells were infected with HCMV at an MOI of 0.1. The extent of virus
724 replication was measured at the indicated times post-infection as described in (B). Results are
725 expressed as means ± SD.
726 **FIG 5** Sliding window analysis of APOBEC3 hotspot motifs along the HCMV genome**.** The HCMV
727 Towne sequence was used (GenBank Accession: GQ121041). Motifs were analyzed in 1000 bp

728 windows moving with a step of 100 bp. For each window, the percentile rank of the real motif count in
729 the distribution of counts from reshuffled windows is plotted. The lower the percentile rank, the fewer
730 motifs are detected in the window when base composition is accounted for (by reshuffling). A
731 schematic representation of HCMV open reading frames (ORFs) is shown with color codes indicating
732 essential ORFs (red), non-essential ORFs (green) and ORFs with unknown effect when deleted (grey).
733
734 **FIG 6** Occurrence of APOBEC3G motif in HCMV. (A) Sliding window analysis of APOBEC3G
735 hotspot motif along the HCMV genome. APOBEC3G motif (CCC) was analyzed for both strands in
736 1000 bp windows moving with a step of 100 bp. For each window, the percentile rank of the real motif
737 count in the distribution of counts from reshuffled windows is plotted. The HCMV Towne sequence
738 was used (GenBank Accession: GQ121041). (B) CCC/CCT motifs comparison. Preference Index
739 calculated for the CCC:GGG motif is plotted against the Preference Index for the CCT:AGG motif,
740 both calculated for Essential (red) and Non Essential (blue) Towne ORFs. Spearman's rank correlation
741 coefficient (rho) is also reported, along with the correlation *P* value.
742
743 **FIG 7** Occurrence of APOBEC3 motifs in HCMV ORFs. (A) The occurrence of hotspot motifs for
744 A3G, A3F/3C and A3A was analyzed by calculating a preference index. Preference indexes are shown
745 in standard box-and-whisker plot representation (thick line: median; box: quartiles; whiskers: 1.5 x
746 interquartile range). The Kruskal-Wallis tests indicated significant differences among motifs
747 ($p<2.2\text{x}10^{-16}$). *P* values from post hoc tests (Nemenyi tests) are shown. N.S., not significant. (B)
748 Occurrence of A3G hotspot motifs in HCMV essential and non-essential ORFs. Essential ORFs have
749 significantly fewer CCC:GGG motifs compared to non-essential ORFs (*P* value from Wilcoxon Rank
750 Sum test). (C) Occurrence of A3G hotspot motifs in different HCMV strains and isolates. The

preference indexes of Towne ORFs are plotted against the corresponding indexes from other HCMV genomes. Isolate derived from different sources or body compartments were analyzed.

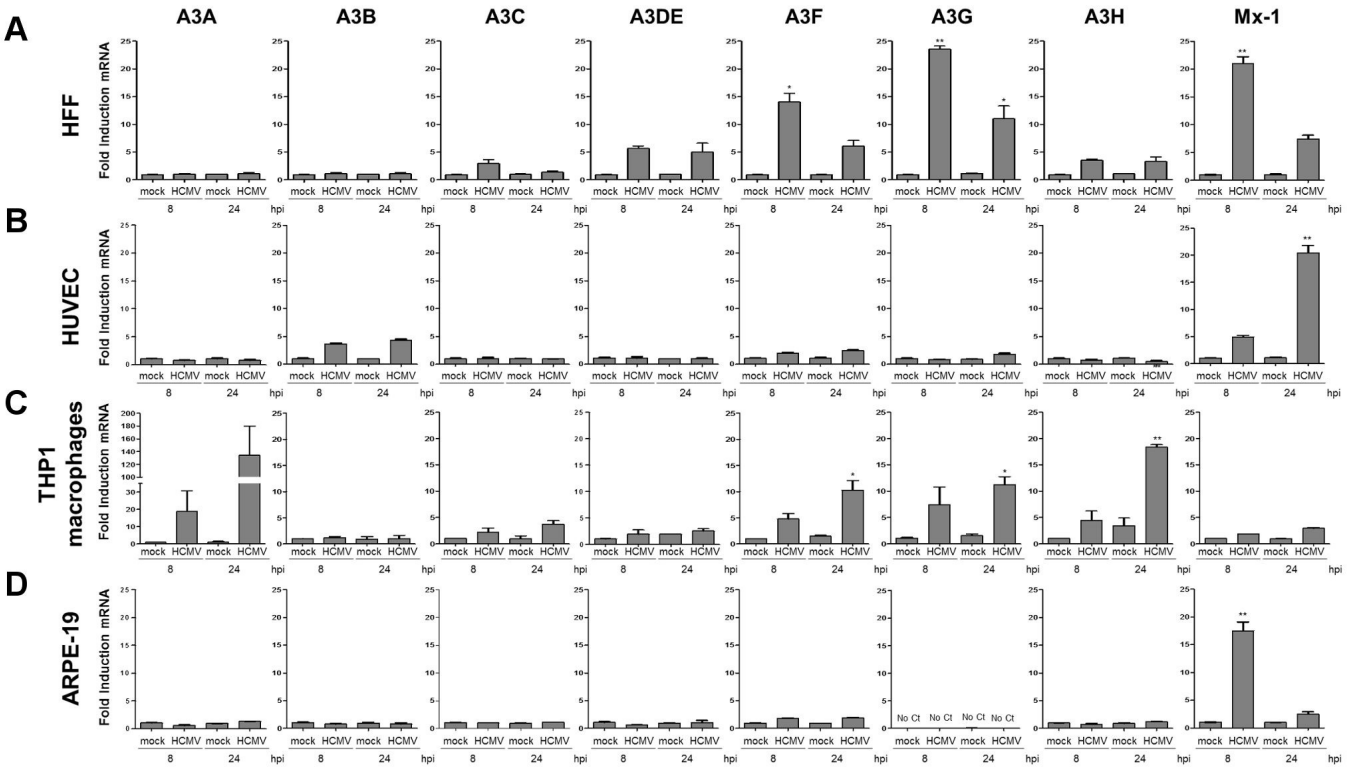

FIGURE 1

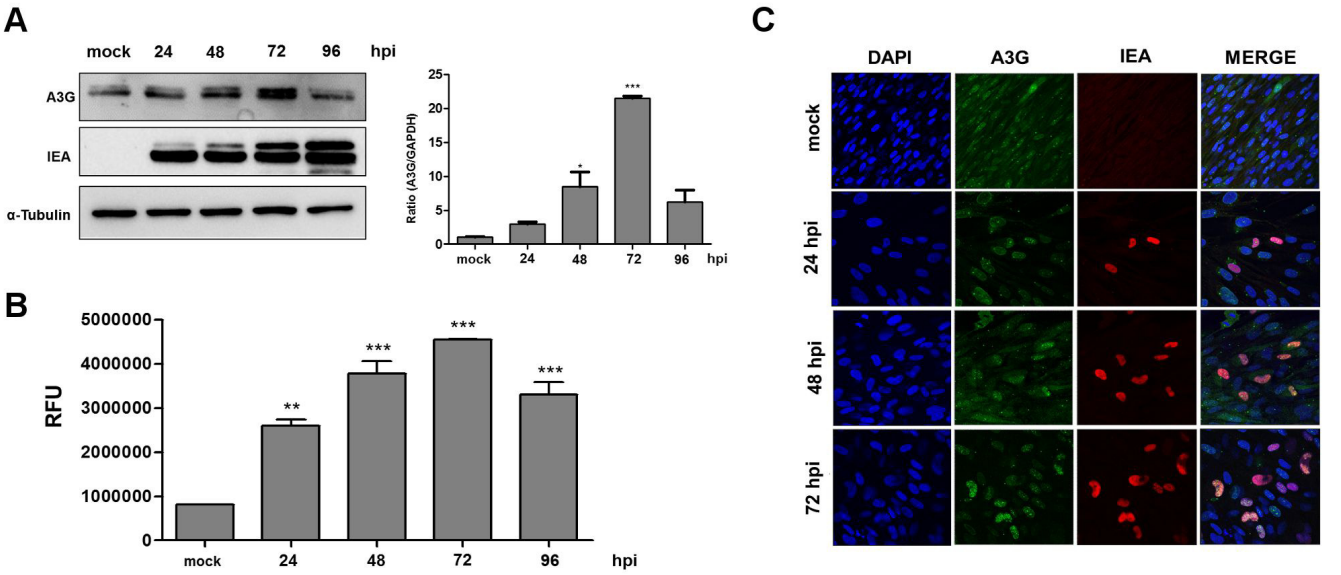

FIGURE 2

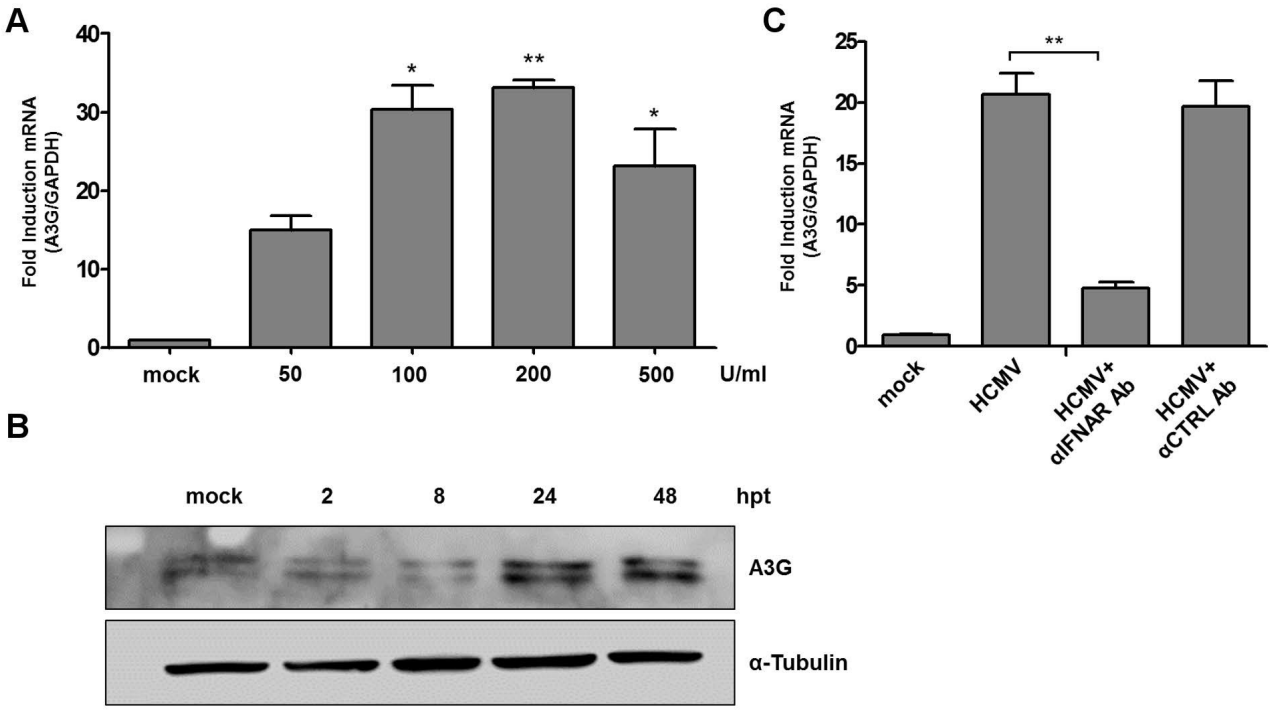

FIGURE 3

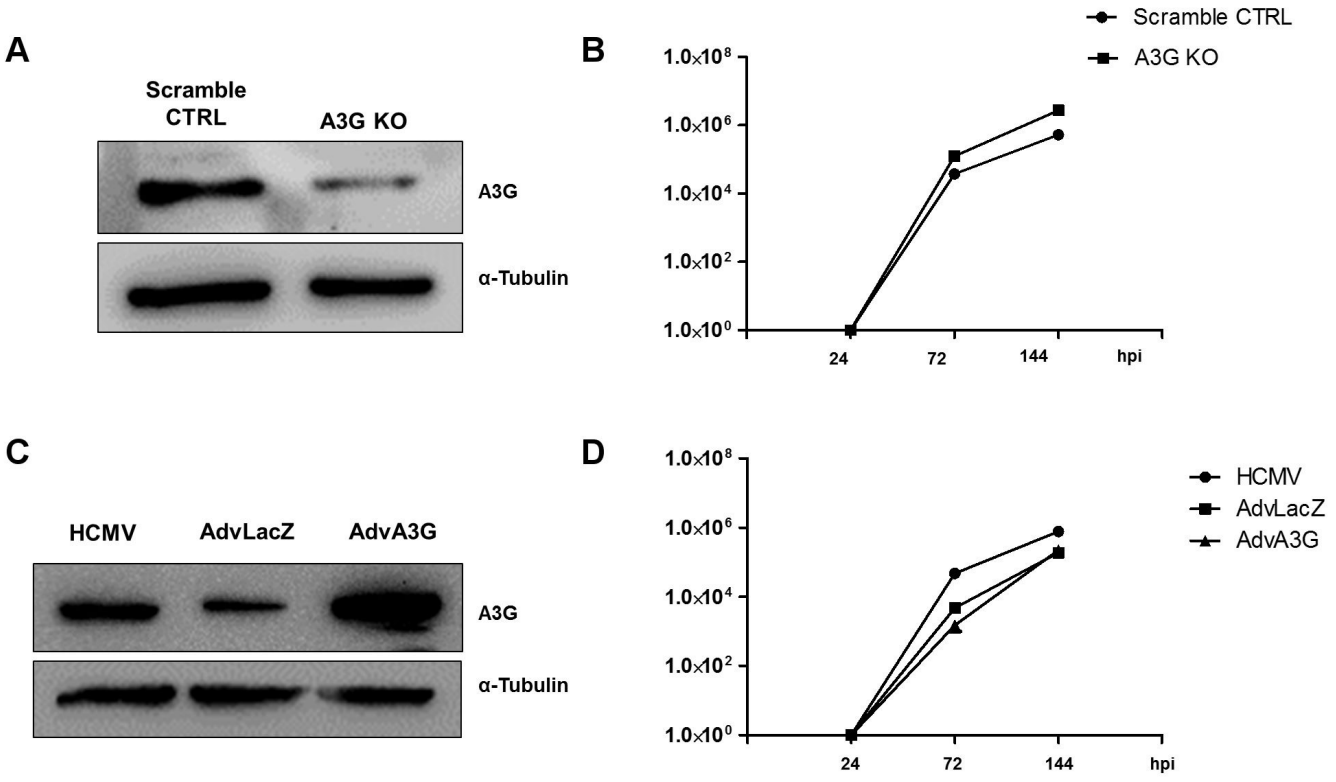

FIGURE 4

Journal of Virology
JVI
Journal of Virology

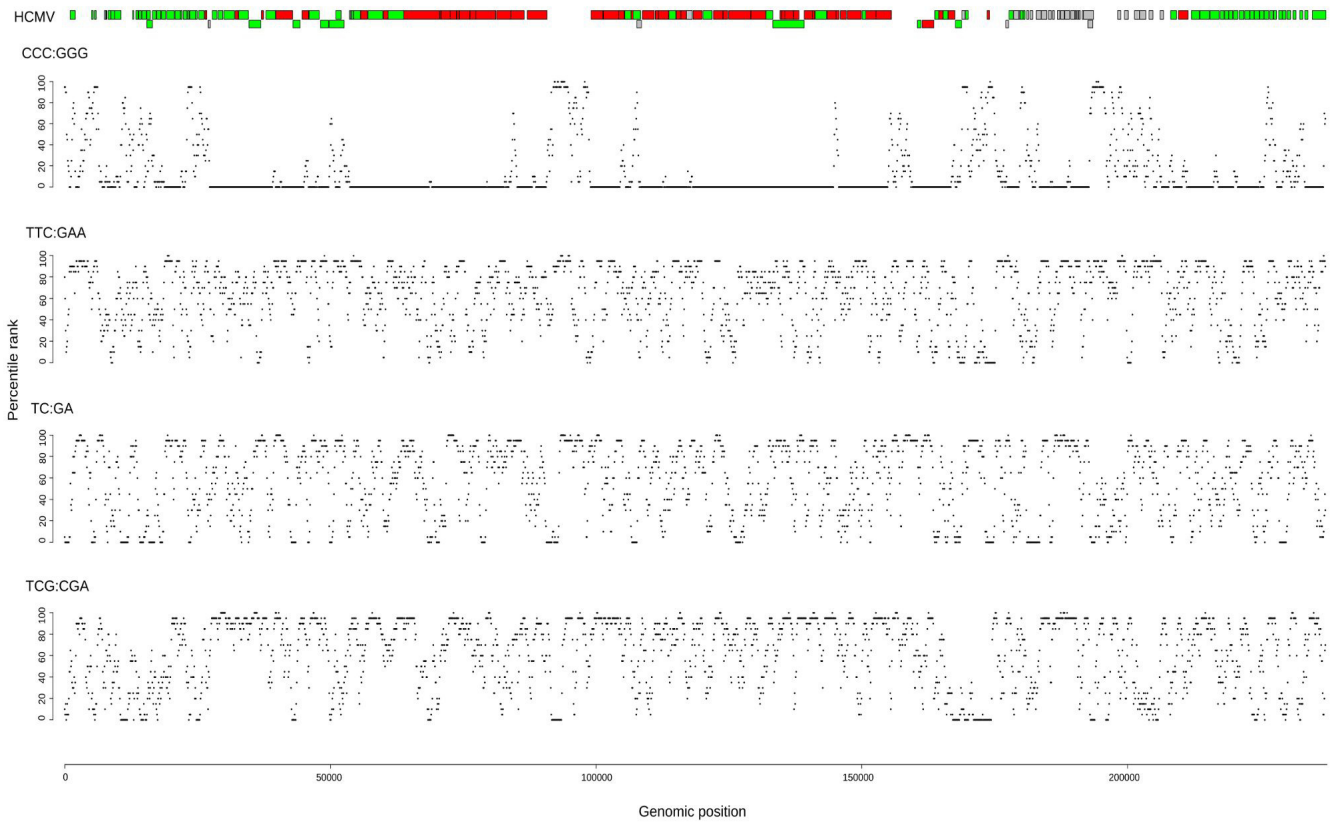

FIGURE 5

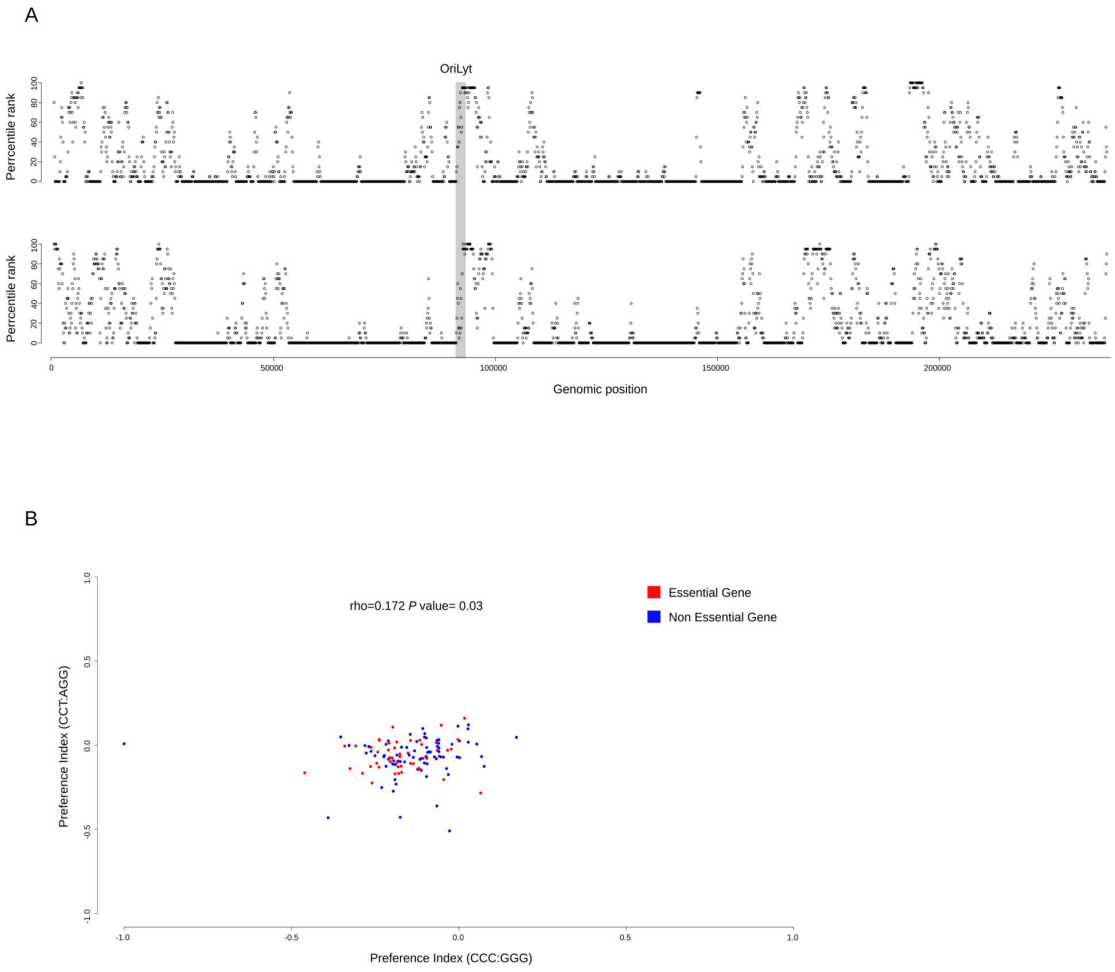

FIGURE 6

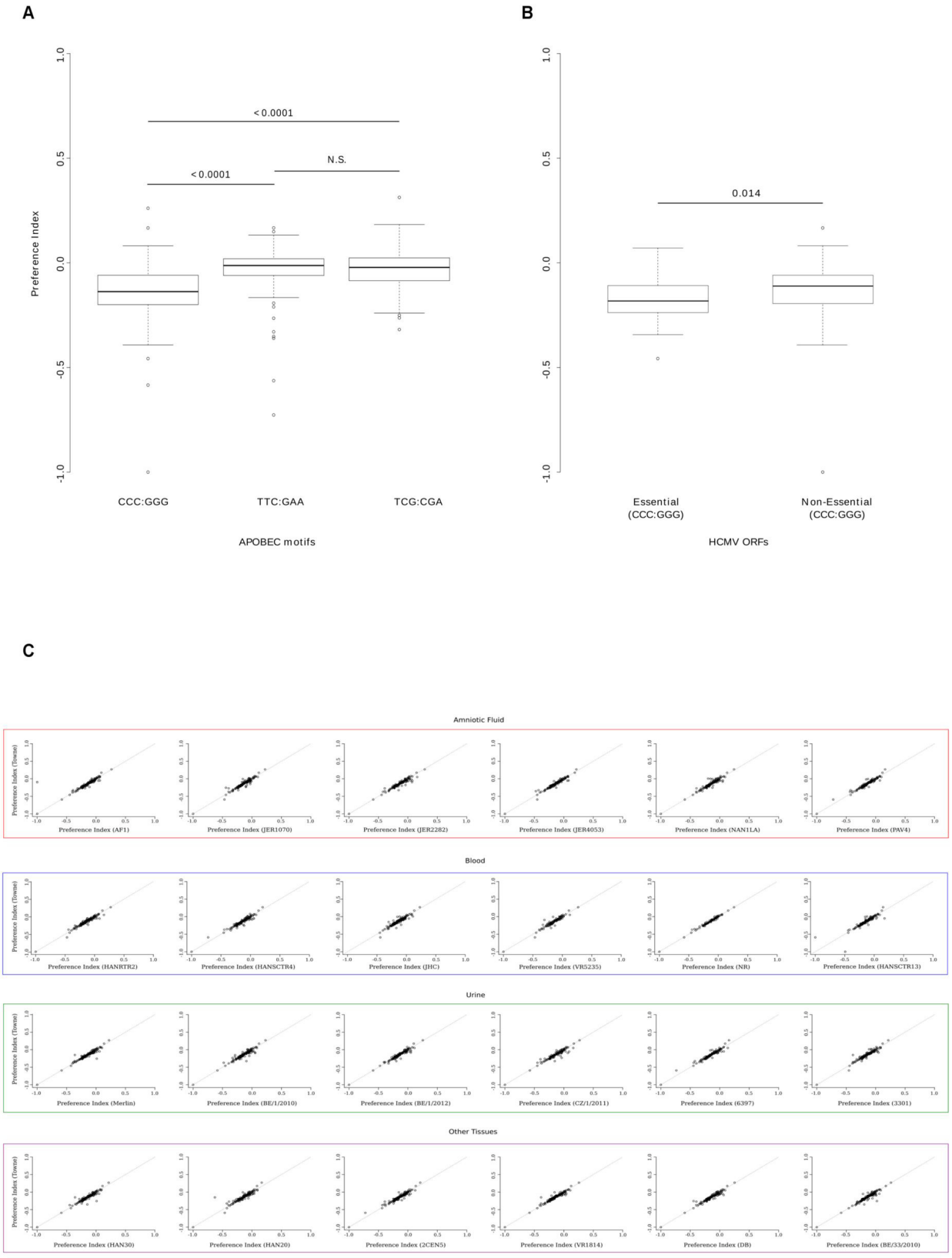

FIGURE 7